

# ALDEHYDE CONTENT OF CELLULOSE DETERMINED BY BENEDICT'S SOLUTION AND VISIBLE ABSORPTION OF COPPER(II)-EDTA COMPLEX

CHING-LEN YU, SIH-HAN JHOU, WEN-SHUO CHENG, SHIH-SYUAN SIAO and  
HAN-YIN CHEN

*Department of Environmental Engineering, Kun Shan University, Yeong Kang District,  
Tainan City 710, Taiwan*

✉ *Corresponding author: Ching-Len Yu, cly@mail.ksu.edu.tw*

*Received October 24, 2018*

Benedict's solution was employed to determine the aldehyde content of a cellulose paper. Benedict's solution, containing Cu(II), citrate and carbonate, is capable of selectively oxidizing the aldehyde groups of cellulose and producing cuprous oxide. The selective oxidation was conducted at room temperature for an extended period of time. The aldehyde content was derived from the change of the Cu(II) concentration. The Cu(II) concentration was determined by measuring the 750 nm radiation absorption of the complex of Cu(II)-ethylene diamine tetraacetic acid (EDTA). The interferences from citrate, carbonate and foreign metallic cations on the 750 nm absorption measurement were also examined. The results showed that the interferences of citrate and carbonate can be removed *via* the dilution of Benedict's solution. Also, the absorption due to the Cu(II)-EDTA complex was observed to be far superior to those of the EDTA complexes of the foreign metallic cations. The foreign metallic cations had a limited interference on the 750 nm absorption measurement. Benedict's solution, together with the 750 nm absorption method, is hence a reliable approach for determining the aldehyde content of cellulose.

**Keywords:** aldehyde content, Benedict's solution, EDTA, photometric titration, visible absorption

## INTRODUCTION

Cellulose is a linear biopolymer, consisting of anhydroglucose repeating units, with two vicinal secondary hydroxyl groups and one primary hydroxyl group per unit.<sup>1</sup> At the one end of the polymer chain, an aldehyde group is located. Aldehyde groups are chemically active and can undergo various reactions, including oxidation and cross-linking. These reactions degrade the quality of cellulose, which becomes yellowish, acidic and brittle. To prolong the shelf-life of cellulose, the aldehyde content should be minimized. Also, if aldehyde groups are promptly transformed into chemically stable functional groups, various specialized cellulose materials and composites can be synthesized for analytical, environmental and industrial applications.<sup>2,3</sup> To increase and control the aldehyde content, several chemical reaction schemes have been suggested and investigated,<sup>4,6</sup> including periodate selective

oxidation of the two vicinal hydroxyl groups. The aldehyde content is crucial for cellulose application and the objective of this study has been to determine the aldehyde content by using Benedict's solution and a visible absorption measurement method. Benedict's solution is a citrate-carbonate alkaline aqueous solution containing Cu(II), capable of selectively oxidizing aldehyde groups.<sup>7,8</sup> The aldehyde content can be derived from the change of the Cu(II) concentration after selective oxidation. This study employed a visible absorption method to determine the Cu(II) concentration of Benedict's solution after the reaction. The visible absorption method utilizes EDTA to react with Cu(II) to form Cu(II)-EDTA complex. Cu(II)-EDTA complex quantitatively absorbs the visible wavelength 750 nm radiation and the Cu(II) concentration after the oxidation can be thus determined from the 750 nm absorbance.<sup>9,10</sup>

The accuracy of the 750 nm absorption method, however, may be affected by two error sources: the foreign metallic ions and the matrices of Benedict's solution. Foreign metallic cations from the cellulose manufacture processes<sup>11,12</sup> may dissolve in Benedict's solution. These metallic cations can react with EDTA to form complexes, which may absorb 750 nm radiation and significantly change the absorbance. Similarly, the matrices of Benedict's solution, including carbonate and citrate, may alter the absorbance of the Cu(II)-EDTA complex. Thus, the 750 nm absorption measurements have to be performed under proper analytical conditions, where the interferences from the two error sources are minimized and negligible. In this study, three methods, including the external method, the minor volume standard addition analysis<sup>10,13</sup> and photometric titration,<sup>14,15</sup> were employed to assure that the 750 nm absorption measurements were not significantly affected by the two error sources. The principles of the three methods are reviewed and outlined in the next section.

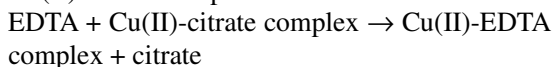
## BACKGROUND

### Benedict's solution

The aldehyde oxidation reaction by Benedict's solution involves two moles of Cu(II)-citrate complex oxidizing one mole of aldehyde groups to produce one mole cuprous oxide precipitates:<sup>7</sup>



Only alcohol groups and ketone groups are not oxidized by Benedict's solution.<sup>7</sup> The aldehyde content can be derived from the change of the Cu(II) concentration. Upon the completion of the oxidation reaction, the Cu(II) concentration of Benedict's solution can be determined by using EDTA to produce the Cu(II)-EDTA complex:<sup>16</sup>



The Cu(II)-EDTA complex strongly absorbs the 750 nm radiation and the absorption behavior complies with the Beer-Lambert law. This absorption property facilitates the determination of the Cu(II) concentration by using a conventional visible absorption spectrometer.

There are, however, several side reactions

competing with Benedict's solution for aldehyde groups. First, Benedict's solution contains high concentrations of carbonate and citrate, which can cause alkaline degradation. Based on the prevailing alkaline degradation mechanism,<sup>17-20</sup> Cannizzaro,  $\beta$ -hydroxycarbonyl elimination, and benzilic acid rearrangement reactions can transform aldehyde groups into various kinds of functional groups. Moreover, the mutarotation reaction can transform the aldehyde group (the reducing end) into a secondary hydroxyl group.<sup>21</sup>

To reduce the occurrence of these side reactions, this study performed the selective oxidation of Benedict's solution at room temperature.<sup>22,23</sup> The reaction period was set for four weeks in order to oxidize as many aldehyde groups as possible.<sup>23</sup> Due to the competition of the side reactions, the aldehyde content determined by this study should be a lower-limit value.

### External method

For the Cu(II) concentrations in the linear range, the 750 nm absorbance  $Y$  of the Cu(II)-EDTA complex can be described by a linear model:<sup>10,15</sup>

$$Y = a + bC_X \quad (1)$$

where  $C_X$  denotes the Cu(II) concentration, the slope  $b$  is the sensitivity, and the intercept  $a$  is the absorbance of the blank. For a sample having an absorbance  $Y_0$ , the Cu(II) concentration  $C_0$  of the sample is determined by Equation 2:

$$C_0 = (Y_0 - a)/b \quad (2)$$

Using Equations 1 and 2 to determine  $C_0$  is known as the external method. If the sample is a diluted one, the Cu(II) concentration  $C_1$  of Benedict's solution equals the resulting  $C_0$  multiplied by a dilution factor. The dilution factor is defined as the total volume of the diluted sample divided by the volume of Benedict's solution in the sample. The purpose of the dilution is to assure that  $Y_0$  of the diluted sample is adequately measurable within the linear range.

### Minor volume standard addition analysis

Benedict's solution contains high concentrations of citrate and carbonate. The citrate and carbonate matrices may significantly change the sample absorbance  $Y_0$ . To take the matrix interferences into account, Equation 1

should be modified as:<sup>10,13</sup>

$$Y = (a + dC_M) + (b + fC_M)C_X \quad (3)$$

where  $C_M$  is the concentration of the matrices,  $dC_M$  represents the intercept type interference, and  $fC_M$  represents the sensitivity type interference. The parameter  $d$  is the sensitivity of the matrices to the 750 nm radiation and the parameter  $f$  is a characteristic value for the strength of the interactions between the matrices and the Cu(II)-EDTA complex. If  $fC_M$  is comparable to  $b$  or  $dC_M$  is notably larger than  $a$ , using Equations 1 and 2 to determine  $C_0$  is obviously inadequate and erroneous.

In practice, however,  $dC_M$  and  $fC_M$  are often unknown. One common approach is to reduce  $C_M$  via sample dilution, which also reduces the magnitudes of  $dC_M$  and  $fC_M$ . Then, using Equations 1 and 2 determines  $C_0$ . However, it is still necessary to examine whether the magnitudes of  $dC_M$  and  $fC_M$  of the diluted sample are sufficiently small and negligible. For  $fC_M$ , its magnitude as compared to  $b$  in Equation 3 can be revealed by performing the minor volume standard addition analysis for both the diluted sample and the blank.<sup>13</sup> The minor volume standard addition analysis is a spiking method, where the spiking volume  $V_S$  of the Cu(II) standard solution is limited within about 1% or less of the diluted sample volume  $V_0$ . The effect of the sample-size increase due to the spiking hence is insignificant. If the Cu(II) concentration of the diluted sample after the spiking is still within the linear range, the total absorbance  $Y_T$  of the spiked diluted samples and  $V_S$  can be described by Equation 4:<sup>13</sup>

$$Y_T = a_1 + b_1 V_S \quad (4)$$

The intercept  $a_1$  and the slope  $b_1$  can be expressed in terms of  $C_0$ , the Cu(II) standard solution concentration  $C_S$ , and the variables and parameters of Equation 3:

$$a_1 = a + dC_M + (b + fC_M)C_0 \quad (5)$$

$$b_1 = (b + fC_M)C_S/V_0 \quad (6)$$

Similarly, the minor volume standard addition analysis is performed for the blank. The absorbance of the spiked blank  $Y_W$  and  $V_S$  can be described by Equation 7:

$$Y_W = a_W + b_W V_S \quad (7)$$

Since both  $dC_M$  and  $fC_M$  equal zero for the blank, the intercept  $a_W$  and the slope  $b_W$  can be expressed in terms of  $C_S$ ,  $b$  and  $V_0$ :

$$a_W = a \quad (8)$$

$$b_W = bC_S/V_0 \quad (9)$$

Under the minor volume addition condition, Equation 7 can be regarded as an alternative expression of Equation 1.

If  $b$  is much larger than  $fC_M$ ,  $b_1$  of Equation 6 should be nearly equal to  $b_W$  of Equation 9. The ratio of Equation 6 and Equation 9 thus reveals the magnitude of  $fC_M$  as compared to  $b$ . We suggested that if the relative slope bias  $B_S$  is within the  $\pm 5\%$  range,  $fC_M$  can be regarded as negligible.<sup>13</sup> Here,  $B_S$  is defined as:

$$B_S = (b_1/b_W - 1) \times 100\% \quad (10)$$

$B_S$  represents the error percentage of  $C_0$  due to  $fC_M$ . If the resulting  $B_S$  value is outside of the  $\pm 5\%$  range, a sample with a larger dilution factor should be prepared and analyzed by the external method and the minor volume standard addition analysis. The dilution and the analysis should continue until  $B_S$  meets the  $\pm 5\%$  criterion. As for  $dC_M$ , its magnitude as compared to  $bC_0$  in Equation 5, however, can not be revealed by the minor volume standard addition analysis in that  $a_1$  of Equation 5 is independent of  $V_S$  and  $C_S$ . Since the effect of  $dC_M$  can not be revealed, this study employed an alternative approach, photometric titration, to eliminate the interference of  $dC_M$ .

### Photometric titration

Photometric titration determines  $C_0$  based on the titration curve, which illustrates the evolution of the absorbance  $Y_P$  of the titrated sample with the accumulative EDTA volume  $V_{E,N}$ .<sup>10,14</sup> For a diluted sample having a volume  $V_0$ ,  $C_0$  is calculated via the following equation:<sup>10</sup>

$$C_0 = C_E V_{E,N}/V_0 \quad (11)$$

where  $V_{E,N}$  is the accumulative EDTA volume at the equivalence point and  $C_E$  is the concentration of the standard EDTA aqueous solution. Clearly, the identification of the equivalence point from the curve is crucial. To accurately identify  $V_{E,N}$ , the photometric titration process has to be carefully designed. In this study,  $V_{E,N}$  is designed to be located at the point where  $Y_P$  reaches its maximum. This design is achieved by meeting the following two conditions: first,  $V_{E,N}$  is strictly limited to the minor volume with respect to  $V_0$ . The sample-volume increase can be treated as negligible. Second, the absorbance of the Cu(II)-EDTA complex at the equivalence point has to be notably larger than the initial absorbance of the Cu(II)-citrate complex. As will be seen later, the present titration curves

showed that this condition is indeed fulfilled.

Once these two conditions are satisfied, it can be shown that  $V_{E,N}$  is located at the point where  $Y_p$  reaches its maximum. The absorbance  $Y_p$  can be expressed as the function of  $V_E$ ,  $C_E$  and the variables and parameters of the matrices given in Equation 3:  $Y_p = (a + dC_M) + A_C(C_0V_0 - C_EV_E)/C_0V_0 + (b + fC_M)C_EV_E/V_0$  (12)

where  $A_C$  is the initial absorbance due to the Cu(II)-citrate complex. Combining Equations 11 and 12 gives:

$$Y_p = (a + dC_M) + A_C(V_{E,N} - V_E)/V_{E,N} + (b + fC_M)C_EV_E/V_0$$

The second term,  $A_C(V_{E,N} - V_E)/V_{E,N}$ , decreases as the titration proceeds. The third term  $(b + fC_M)C_EV_E/V_0$  represents the absorbance of the Cu(II)-EDTA complex and this term increases as  $V_E$  increases. Upon arriving at the equivalence point (*i.e.*,  $V_E = V_{E,N}$ ), the second term vanishes. If  $(b + fC_M)C_EV_{E,N}/V_0$  is greater than  $A_C$  (the second condition),  $Y_p$  reaches its maximum. Namely,  $V_{E,N}$  is located at the point having a maximal value of  $Y_p$ . Also, from Equation 13, although  $Y_p$  is a function of  $fC_M$  and  $dC_M$ ,  $V_{E,N}$  is independent from the magnitudes of  $fC_M$  and  $dC_M$ . Hence,  $C_0$  determined by Equation 11 is not influenced by  $fC_M$  and  $dC_M$ .

### Foreign metallic cation interference

The participation of foreign metallic cations in the EDTA complex chemistry can greatly complicate data analysis: Not only do foreign metallic cations compete with Cu(II) for EDTA, but their complexes of EDTA and other anions likely also absorb the 750 nm radiation.<sup>10,16</sup> This study examined the interference of foreign metallic cations by adding the foreign metallic cations into the diluted sample of Benedict's solution. The 750 nm absorption measurements of the diluted sample were then conducted at the pH value of either 5 (using an acetate buffer) or 7 (using a phosphate buffer). At these two pH values, the Cu(II)-EDTA complex has a conditional stability constant greater than those of most metallic cations-EDTA complexes.<sup>10</sup> The competition of foreign metallic cations with Cu(II) for EDTA was inhibited. The apparent Cu(II) concentration  $C_2$  of Benedict's solution with the presence of the foreign metallic cations was determined by the external method and photometric titration. By comparing  $C_2$  with  $C_1$ ,

the effect of the foreign metallic cations was discovered.

## EXPERIMENTAL

### Chemicals and Benedict's solution

The chemicals used in this study were purchased from Panreac, Sigama-Aldrich, Merck, Showa Chemicals and Shimakyu's Pure Chemicals. The deionized water produced by Roda Ultrapur Water, Taiwan, was employed for all of the aqueous solution preparations. Benedict's solution was prepared by the following procedure: 10 g of sodium carbonate anhydrous and 17.3 g of sodium citrate 2-hydrate were dissolved in 90 mL deionized water and 0.346 g of copper sulphate 5-hydrate was dissolved in 10 mL deionized water. Upon full dissolution, the copper sulphate solution was added slowly drop-by-drop into the sodium carbonate-sodium citrate solution stirred by a magnetic stirrer (Corning PC320). The initial Cu(II) concentration of Benedict's solution was 878.8 mg/L.

The cellulose sample was a commercial copy paper. Three grams of the paper sample were cut into pieces of a size range from 0.7 to 1.0 cm. The paper fragments were immersed into 50 mL of Benedict's solution. The solution stood at room temperature for at least four weeks. Upon the completion of the oxidation, Benedict's solution and the paper fragments were separated by vacuum filtration, using a Pall glass fiber filter. The Cu(II) concentration of Benedict's solution was then analyzed by the external method, the minor volume standard addition, and photometric titration.

### External method

Standard Cu(II) solutions were prepared in six 50 mL volumetric flasks, using a 5000 mg/L Cu(II) standard solution. For each volumetric flask, various volumes (0.0, 0.4, 0.8, 1.2, 1.6, or 2.0 mL) of the Cu(II) standard solution were added, followed by 10 mL of 0.025 M EDTA solution. The EDTA solution was prepared by using ethylenediamine tetraacetic acid disodium salt dihydrate. The mole ratio of EDTA to Cu(II) was at least 26 fold or higher. The pH value of the standard Cu(II) solutions was then adjusted by adding 35 mL of the phosphate buffer (or the acetate buffer), followed by 5 mL deionized water.

The sample was prepared by mixing 5 mL of Benedict's solution, 10 mL of 0.025 M EDTA solution, and 35 mL of the phosphate buffer in a 50 mL volumetric flask. The dilution factor for Benedict's solution was thus ten. The 750 nm absorbance of the standard solutions and the sample was measured by a Labomed Spectro UV-VIS Double spectrometer, with a glass cell of 10 mm inner width.

Phosphate buffer having a pH value of 7.42 was prepared by mixing 34.0 g of potassium di-hydrogen phosphate and 10 g sodium hydroxide in an aqueous solution of a total volume of 500 mL. The acetate buffer having a pH value of 4.83 was prepared by mixing 23.0 g of sodium acetate anhydrous and 7.2 mL of acetic acid in an aqueous solution of a total volume of 500 mL. The pH values were measured by a TOA-DKK HM30 pH meter.

#### Minor volume standard addition analysis

Five samples were prepared by mixing 5 mL of Benedict's solution, 10 mL of 0.025 M EDTA solution, and 35 mL of the acetate buffer (or the phosphate buffer) in 50 mL volumetric flasks. The five samples were then spiked by the 5000 mg/L Cu(II) standard solution with five different volumes: 0.0 (without spiking), 0.5, 1.0, 1.5, and 2.0 mL. The 750 nm absorbance of the spiked samples was measured by the spectrometer. Six blanks were prepared by mixing 5 mL of deionized water, 10 mL of 0.025 M EDTA solution, and 35 mL of the acetate buffer (or the phosphate buffer) in 50 mL volumetric flasks. The blanks were then spiked by the 5000 mg/L Cu(II) standard solution with six different volumes: 0.0, 0.5, 1.0, 1.5, 2.0 and 2.5 mL. The 750 nm absorbance of the spiked blanks was then measured by the spectrometer.

#### Photometric titration

The sample was prepared by mixing 5 mL of Benedict's solution, 35 mL of the buffer and 5 mL of deionized water in a 100 mL Erlenmeyer flask. The sample was then stirred by the magnetic stirrer with a constant speed. The sample was titrated by a 0.050 M or 0.025 M EDTA solution *via* a burette. After titrating 0.05 mL of the EDTA solution and stirring for a while, the absorbance of the titrated sample was measured by the spectrometer. The titration and the absorbance measurements were continuously performed for at least 3 mL of the accumulative EDTA volume titrated into the sample and a peak-shape curve was observed.

#### Foreign metallic cation interference

The sample was prepared in a 50 mL volumetric flask by mixing 5 mL of Benedict's solution, 10 mL of 0.025 M EDTA solution, 32 mL of the buffer, and 3 mL of a foreign metallic cation aqueous solution having a concentration of 1000 mg/L. The sample hence contained 60 mg/L of the foreign metallic ions. The sample was analyzed by the external method, as described above. The compounds used for the preparation of the foreign metallic cations were silver(I) nitrate, aluminum(III) sulfate octadecahydrate, calcium(II) carbonate, cobalt(II)

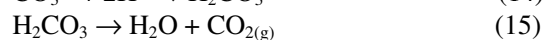
chloride hexahydrate, ammonium iron(II) sulfate hexahydrate, ferric nitrate nonahydrate, magnesium(II) carbonate basic, manganese(II) sulfate monohydrate, nickel(II) sulfate hexahydrate, lead(II) nitrate, and zinc(II) sulfate heptahydrate.

The sample containing Ni(II) for photometric titration was prepared in a 50 mL volumetric flask by mixing 5 mL of Benedict's solution, 5 mL of deionized water, 33 mL of the phosphate buffer, 2 mL of Ni(II) aqueous solution having a concentration of 1000 mg/L. The sample hence contained 44.4 mg/L of Ni(II). The sample containing Pb(II) was prepared in a 50 mL volumetric flask by mixing 5 mL of Benedict's solution, 5 mL of deionized water, 32 mL of the phosphate buffer, and 3 mL of Pb(II) aqueous solution having a concentration of 1000 mg/L. The sample thus contained 66.7 mg/L of Pb(II). Both samples were then titrated by a 0.025 M EDTA solution.

## RESULTS AND DISCUSSION

The linear models (Eq. 1) of the 750 nm absorption of the Cu(II)-EDTA complex are given in Table 1. The correlation coefficient  $R_C$  values of the models are higher than 0.995. The slope values of the linear models of the two buffers are in very close agreement. The resulting linear models confirmed that the 750 nm absorption of the Cu(II)-EDTA complex obeys the Beer-Lambert law. The molar absorption coefficient of the Cu(II)-EDTA complex was calculated to be  $92 \text{ cm}^2 \text{ mol}^{-1}$ . If the minimal absorbance requirement was 0.005 (1% loss of the transmittance), the lowest measurable Cu(II) concentration was estimated to be about 4 mg/L.

Table 1 also lists  $C_1$  of two replicas determined by Equation 2. For the phosphate buffer case, two  $C_1$  replicas are in close agreement. As for the acetate buffer case, the difference of two  $C_1$  replicas reached 90 mg/L. This difference caused a two-fold uncertainty on the aldehyde content, as shown in Table 1. The difference mainly resulted from the light scattering of carbon dioxide tiny gas bubbles. Carbon dioxide was produced from the carbonate matrix in the acidic condition *via* the following reactions:<sup>24</sup>



Carbon dioxide gas bubbles were observed randomly dispersing in the glass cell during the visible absorption measurements. Light

scattering by the tiny gas bubbles increased the absorbance, which caused the 90 mg/L difference between the two  $C_1$  replicas.

Carbon dioxide gas bubbles also caused notable interference (data scatter) in the minor volume standard addition analysis. Table 2 lists Equation 4 for the spiked samples, Equation 7 for the spiked blanks,  $R_C$  of the two equations, and the slope bias  $B_S$ . For the acetate buffer case,  $R_C$  (0.978) of Equation 4 is smaller than that (0.999) of Equation 7. The smaller  $R_C$  value reflects a relatively larger data scatter of  $Y_T$  than that of  $Y_W$ , as depicted in Figure 1. Moreover, the  $B_S$  value reaches 8.6%. Since the interference of carbon dioxide gas bubbles was random, its quantitative effect was not included in Equations 1 and 3. The absorption measurements thus had to be performed in a slightly basic condition such as in the phosphate buffer in order to inhibit the generation of carbon dioxide gas bubbles. Table 2 shows  $R_C$  of Equations 4 and 7 and  $B_S$  for the phosphate buffer. Without the interference from carbon dioxide gas bubbles, the two  $R_C$  values are higher than 0.995 and the  $B_S$  value is less than 1%. The low  $B_S$  value indicated that the sensitivity type interference  $fC_M$  was removed by a dilution factor of ten for the Benedict's solution sample.

Figure 2 shows the photometric titration curve of the sample in the phosphate buffer. A maximal absorbance value of 0.12, mainly due

to the absorption of the Cu(II)-EDTA complex, was observed at  $V_E$  of 1.10 mL. This value is greater than the initial absorbance value (0.072), which was mainly due to the absorption of the Cu(II)-citrate complex. Since the two conditions were satisfied, based on Equation 13, the equivalence point  $V_{E,N}$  was located at 1.10 mL. From Equation 11,  $C_1$  was calculated to be 698.5 mg/L. This value is in close agreement with those of the external method (Table 1). In other words,  $C_1$  determined by the external method was not affected by  $fC_M$  and  $dC_M$ . Therefore, a dilution factor of ten for Benedict's solution was sufficient to remove both matrix interferences. The average of  $C_1$  determined by the photometric titration and the external method is 692.6 mg/L. The Cu(II) loss due to the selective oxidation reaction was  $1.47 \times 10^{-4}$  mol.

The aldehyde content was thus determined to be  $2.44 \times 10^{-5}$  mol per gram of the paper. This value is in agreement with several recent published data.<sup>25-28</sup>

Table 3 gives  $C_2$  and the apparent aldehyde content of the sample, determined by the external method in the phosphate buffer with the presence of various foreign metallic cations. Also, it lists the relative difference between  $C_2$  and the  $C_1$  average (692.6 mg/L). The relative difference values of most foreign metallic cations are less than 8%, except that of the Ni(II) case.

Table 1  
Linear models and aldehyde contents determined by the external method

Buffer	Phosphate	Acetate
Equation 1	$Y = 1.450 \times 10^{-3} C_X - 1.50 \times 10^{-3}$	$Y = 1.438 \times 10^{-3} C_X + 1.10 \times 10^{-3}$
$R_C$ of Equation 1	0.995	0.999
$C_0$ (mg/L)	68.62	68.78
$C_1$ (mg/L)	686.2	687.8
Aldehyde content	$2.53 \times 10^{-5}$	$2.51 \times 10^{-5}$

Table 2  
Minor volume standard addition analysis for the samples and the blanks

Buffer	Phosphate	Acetate
Equation 4	$Y_T = 0.1403 V_S + 0.0968$	$Y_T = 0.1486 V_S + 0.0998$
$R_C$ of Equation 4	0.999	0.978
Equation 7	$Y_W = 0.1394 V_S - 0.0001$	$Y_W = 0.1369 V_S + 0.0034$
$R_C$ of Equation 7	0.995	0.999
$B_S$ of Equation 10	0.65%	8.55%

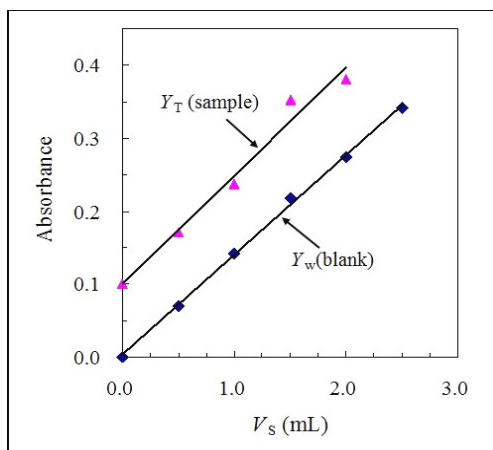


Figure 1: Minor volume standard addition analyses for the sample and the blank in the acetate buffer

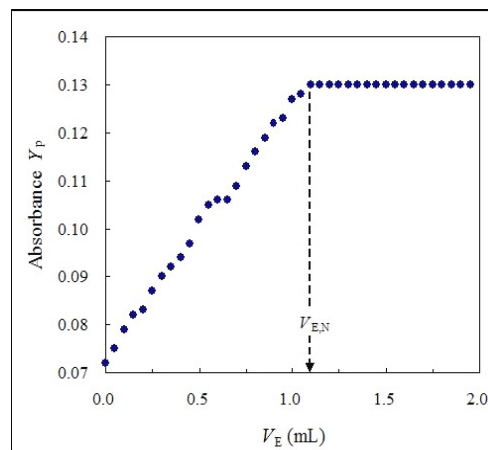


Figure 2: Photometric titration curve for the sample titrated by an EDTA solution of 0.050 M with the equivalence point  $V_{E,N}$  at 1.10 mL

Table 3  
Apparent aldehyde content determined by the external method in the phosphate buffer

Metallic ions	$C_2$ (mg/L)	Relative difference to $C_1$ average (%)	Apparent aldehyde content (mol/g)	Error (%)
Ag(I)	700.0	1.1	$2.35 \times 10^{-5}$	-3.8
Al(III)	713.8	3.1	$2.17 \times 10^{-5}$	-11.3
Ca(II)	706.9	2.1	$2.26 \times 10^{-5}$	-7.5
Co(II)	706.9	2.1	$2.26 \times 10^{-5}$	-7.5
Fe(II)	727.6	5.1	$1.98 \times 10^{-5}$	-18.7
Fe(III)	679.3	-1.9	$2.62 \times 10^{-5}$	7.3
Mg(II)	713.8	3.1	$2.17 \times 10^{-5}$	-11.3
Mn(II)	706.9	2.1	$2.26 \times 10^{-5}$	-7.5
Ni(II)	782.8	13.0	$1.26 \times 10^{-5}$	-48.4
Pb(II)	748.3	8.0	$1.71 \times 10^{-5}$	-29.8
Zn(II)	748.3	8.0	$1.71 \times 10^{-5}$	-29.8

The absorption of the 750 nm radiation by the Cu(II)-EDTA complex is therefore very selective in comparison with most foreign metallic cations. The resulting apparent aldehyde contents are in the range from  $1.26 \times 10^{-5}$  to  $2.62 \times 10^{-5}$  mol/g, as shown in Table 3. As compared to the aldehyde content ( $2.44 \times 10^{-5}$  mol/g) of the sample without foreign metallic ions, the errors of most cases are less than  $\pm 30\%$ , except that the Ni(II) case has an error of  $-49\%$ . Thus, in the presence of various metallic cations, Benedict's solution, in conjunction with the 750 nm absorption method, is still able to determine the aldehyde content up to a reasonable level of accuracy.

Table 4 gives  $C_2$  and the apparent aldehyde content of the sample, determined by the external method in the acetate buffer with the presence of various foreign metallic cations. Due

to the interferences of light scattering of carbon dioxide gas bubbles and the absorption of the EDTA complexes of the foreign metallic cations, most of the relative difference between  $C_2$  and the  $C_1$  average are notably larger than those of Table 3. Similarly, most of the apparent aldehyde contents have larger errors and exhibit a six-fold uncertainty.

Although photometric titration is capable of eliminating matrix interferences, the presence of some foreign metallic cations in the sample can distort the photometric titration curve. Under this circumstance, using the maximal absorbance (Eq. 13) to identify the equivalence point of the distorted titration curves could result in larger errors. Figure 3 shows two distorted titration curves for the Ni(II) and Pb(II) cases in the phosphate buffer. The distortions of these two curves were caused by the 750 nm absorption of

the Ni(II)-EDTA complex and light scattering by the fine particles lead hydrogen phosphate  $\text{Pb}(\text{HPO}_4)$ . Table 5 summarizes the resulting  $C_2$  and the apparent aldehyde content of the two distorted titration curves. For the purpose of comparison, Table 5 also lists  $C_1$  derived from the titration curve of Figure 2 and the aldehyde content derived from the  $C_1$  average.

The lower curve (triangle symbols) of Figure 3 is the titration curve of the Cu(II) and Ni(II) coexisting sample having a Ni(II) concentration of 44.4 mg/L. The curve shape and absorbance values are similar to that of Figure 2. However, due to the weak absorption of the Ni(II)-EDTA complex, rather a deflection point (not a maximum) appeared at  $V_E$  of 2.30 mL. The presence of Ni(II) in the sample did not notably change the titration chemistry: Cu(II) was

greatly favored by EDTA and the Ni(II)-EDTA complex formed in the later part of the titration process. The deflection point was an indication of the transition of the EDTA complex chemistry from Cu(II) to Ni(II). Assuming that  $V_{E,N}$  equaled 2.30 mL,  $C_2$  was calculated to be 730.3 mg/L, which has a relative difference of 5.4% in comparison with the  $C_1$  average. The difference mainly resulted from the fact that after most Cu(II) had reacted with EDTA, the competition of Ni(II) for EDTA slightly delayed the arrival of the equivalence point. The apparent aldehyde content was thus  $1.95 \times 10^{-5}$  mol/g and the error – about -20%.

The upper curve (rhombus symbols) of Figure 3 is the titration curve of the Cu(II) and Pb(II) coexisting sample having a Pb(II) concentration of 66.7 mg/L.

Table 4  
Apparent aldehyde content determined by the external method in the acetate buffer

Metallic ions	$C_2$ (mg/L)	Relative difference to $C_1$ average (%)	Apparent aldehyde content (mol/g)	Error (%)
Ag(I)	993.7	43.5	$-1.51 \times 10^{-5}$	-
Al(III)	757.3	9.3	$1.59 \times 10^{-5}$	-34.7
Ca(II)	847.7	23.0	$4.08 \times 10^{-6}$	-83.3
Co(II)	743.4	7.3	$1.78 \times 10^{-5}$	-27.2
Fe(II)	722.5	4.3	$2.05 \times 10^{-5}$	-15.9
Fe(III)	673.9	-2.7	$2.69 \times 10^{-5}$	10.2
Mg(II)	736.4	6.3	$1.87 \times 10^{-5}$	-23.4
Mn(II)	833.8	20.4	$5.91 \times 10^{-6}$	-75.8
Ni(II)	708.6	2.3	$2.23 \times 10^{-5}$	-8.5
Pb(II)	889.4	28.4	$-1.39 \times 10^{-6}$	-
Zn(II)	819.9	18.4	$7.73 \times 10^{-6}$	-68.3

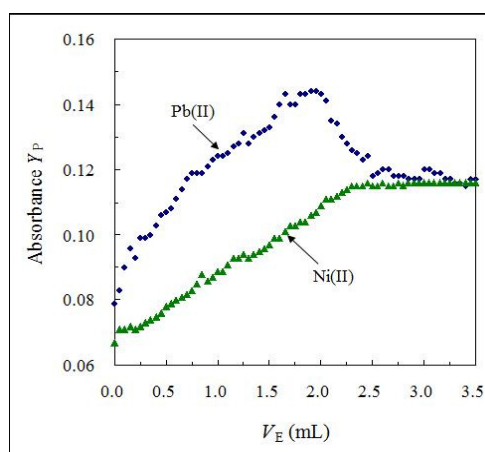


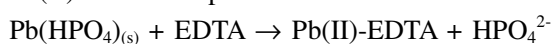
Figure 3: Photometric titration curves of the sample with Ni(II) of 44.4 mg/L (the lower with triangle symbols) and the sample with Pb(II) of 66.7 mg/L (the upper with rhombus symbols)

Table 5  
Apparent aldehyde content determined by the photometric titration in the presence of Ni(II) and Pb(II)

Titration curves	Triangle symbols of Figure 3	Rhombus symbols of Figure 3
Metallic ion species titrated	Cu(II), Ni(II)	Cu(II), Pb(II)
$C_E$ (M)	0.025	0.025
$V_{E,N}$ (mL)	2.30	2.00
$C_2$ (mg/L)	730.3	635.0
Relative difference of $C_2$ to $C_1$ average (%)	5.4	-8.4
Apparent aldehyde content (mol/g)	$1.95 \times 10^{-5}$	$3.20 \times 10^{-5}$
Error (%)	-20.1	31.1

The curve shape and absorbance values are very distinct from those of the Cu(II) and Ni(II) coexisting sample (the lower). Furthermore, before the titration started, the initial absorbance was higher than that of the lower. The higher initial absorbance values resulted from severe light scattering of the 750 nm radiation by white fine particles, lead hydrogen phosphate  $Pb(HPO_4)$ .<sup>10</sup> The  $Pb(HPO_4)$  fine particles formed instantaneously once adding the Pb(II) solution into the sample. Moreover, the fine particles were found nearly uniformly suspended in the sample with a slow settling rate. The slow settling phenomenon was due to the fact that the citrate matrix separated the fine particles and decelerated particle growth, aggregation and precipitation.<sup>10,24</sup> Besides Pb(II), Ba(II), Co(II) and Sr(II) also form particles in the  $HPO_4^{2-}$  aqueous solution.<sup>10,16</sup>

As the titration proceeded, the sample absorbance increased and  $Pb(HPO_4)$  fine particles were still visibly suspended in the sample. This indicated that the formation of the Cu(II)-EDTA complex was favored. The titration curve reached its maximum at  $V_E$  of 2.00 mL. In the range from 2.00 mL to 2.50 mL, the  $Pb(HPO_4)$  fine particles started disappearing and the sample absorbance drastically decreased. Upon  $V_E$  greater than 2.50 mL, the color of the titrated sample became transparently turquoise and the  $Pb(HPO_4)$  fine particles disappeared. The absorbance was approximately steady. The disappearance of the  $Pb(HPO_4)$  fine particles mainly resulted from the formation of the Pb(II)-EDTA complex:



The drastic decrease of the absorbance was attributed to two causes. First, the light scattering phenomenon was lessened by the

disappearance of the  $Pb(HPO_4)$  fine particles. Second, the 750 nm absorbance due to the newly formed Pb(II)-EDTA complex was weak, as shown in Table 3. The starting decrease of the absorbance right beyond  $V_E$  of 2.00 mL was also an indication of the transition of the EDTA complex chemistry from Cu(II) to Pb(II). Assuming that  $V_{E,N}$  equaled 2.00 mL, the resulting  $C_2$  was 635.0 mg/L, which had a relative difference of -8.4%, as compared to the  $C_1$  average. The negative relative difference implied that a small portion of Cu(II) adsorbed onto the  $Pb(HPO_4)$  fine particles. The apparent aldehyde content was calculated to be  $3.20 \times 10^{-5}$  mol/g, which has an error of 31%.

## CONCLUSION

This study employed Benedict's solution to determine the aldehyde content of a cellulose paper. The Cu(II)-citrate complex of Benedict's solution is capable of selectively oxidizing aldehyde groups. To reduce the competition of side reactions, this study performed the oxidation reaction at room temperature for a period of four weeks. The aldehyde content was derived from the change of the Cu(II) concentration of Benedict's solution by using the 750 nm absorption of the Cu(II)-EDTA complex. The carbonate and citrate matrices of Benedict's solution and foreign metallic cations might however cause significant interferences on the 750 nm absorption method. This study employed the sample dilution to remove the matrix interferences. The effects of the matrix interferences were examined by the minor volume standard addition analysis and photometric titration. The results showed that a dilution factor of ten for Benedict's solution was sufficient to remove the matrix interferences. Moreover, to eliminate the scattering of the 750

nm radiation by the carbon dioxide gas bubbles, which were produced from the carbonate matrix under the acidic condition, the 750 nm absorption measurements could only be performed under the basic condition. This study also observed that in the presence of various foreign metallic cations, the 750 nm radiation was still selectively absorbed by the Cu(II)-EDTA complex. This highly selective absorption property enables the determination of the aldehyde content to reach a reasonable accuracy, even if a cellulose sample contains various foreign metallic cations. In summary, Benedict's solution, together with the 750 nm absorption method, is very suitable for determining the aldehyde content of cellulose.

## REFERENCES

- <sup>1</sup> R. H. Atalla and A. Isogai, in "Comprehensive Natural Products II", Vol. 6, edited by L. Mander and H. W. Liu, Elsevier Inc., 2010, pp. 493-539, <https://doi.org/10.1016/B978-008045382-8.00691-2>
- <sup>2</sup> C. Ruiz-Palmero, M. L. Soriano and M. Valcárcel, *Trends Anal. Chem.*, **87**, 1 (2017), <https://doi.org/10.1016/j.trac.2016.11.007>
- <sup>3</sup> D. Q. Melo, V. O. S. Neto, F. C. F. Barros, G. S. C. Raulino, C. B. Vidal *et al.*, *J. Appl. Polym. Sci.*, **133**, 43286 (2016), <https://doi.org/10.1002/app.43286>
- <sup>4</sup> S. Coseri, G. Biliuta, B. C. Simionescu, K. Stana-Kleinschek, V. Ribitsch *et al.*, *Carbohydr. Polym.*, **93**, 207 (2013), <https://doi.org/10.1016/j.carbpol.2012.03.086>
- <sup>5</sup> K. A. Kristiansen, A. Potthast and B. E. Christensen, *Carbohydr. Res.*, **345**, 1264 (2010), <https://doi.org/10.1016/j.carres.2010.02.011>
- <sup>6</sup> G. Pierre, C. Punta, C. Delattre, L. Melone, P. Dubessay *et al.*, *Carbohydr. Polym.*, **165**, 71 (2017), <https://doi.org/10.1016/j.carbpol.2017.02.028>
- <sup>7</sup> R. L. Shriner, R. C. Fuson, D. Y. Curtin and T. C. Morrill, "The Systematic Identification of Organic Compounds", 6<sup>th</sup> ed., John Wiley Inc., 1980, p. 172, <https://www.wiley.com>
- <sup>8</sup> R. Dash, T. Elder and A. Ragauskas, *Cellulose*, **19**, 2069 (2012), <https://doi.org/10.1007/s10570-012-9769-2>
- <sup>9</sup> P. B. Sweetser and C. E. Bricker, *Anal. Chem.*, **25**, 253 (1953), <https://doi.org/10.1021/ac60074a012>
- <sup>10</sup> I. M. Kolthoff, E. B. Sandell, E. J. Meehan and S. Bruckenstein, "Quantitative Chemical Analysis", 4<sup>th</sup> ed., Macmillan Inc., 1969, 1139 p. <https://www.macmillanlearning.com>
- <sup>11</sup> G. Mertoglu-Elmas and G. Cinar, *BioResources*, **13**, 7560 (2018), <https://doi.org/10.15376/biores.13.4.7560-7580>
- <sup>12</sup> M. A. Hubbe and M. A. Gill, *BioResources*, **11**, 2886 (2016), <https://doi.org/10.15376/biores.11.1.2886-2963>
- <sup>13</sup> C.-L. Yu, *J. Technol.*, **29**, 27 (2014), <http://jt.ntust.edu.tw/index.php/jot>
- <sup>14</sup> M. A. Leonard, in "Comprehensive Analytical Chemistry", Vol. 8, edited by G. Svehla, Elsevier Inc., 1977, pp. 207-389, <https://www.sciencedirect.com/handbook/comprehensive-analytical-chemistry>
- <sup>15</sup> D. A. Skoog, F. J. Holler and S. R. Crouch, "Principles of Instrumental Analysis", 6<sup>th</sup> ed., Brooks/Cole-Thomson Learning Inc., 2007, 1056 p., <https://www.cengage.com/c/principles-of-instrumental-analysis-6e-skoog>
- <sup>16</sup> A. E. Martell and R. M. Smith, "Critical Stability Constants", Vols. 1-6, Plenum Press Inc., 1989, <https://doi.org/10.1007/978-1-4615-6764-6>
- <sup>17</sup> K. Rahn and Th. Heinze, *Cellulose Chem. Technol.*, **32**, 173 (1998), <http://www.cellulosechemtechnol.ro>
- <sup>18</sup> C. J. Knill and J. F. Kennedy, *Carbohydr. Polym.*, **51**, 281 (2003), [https://doi.org/10.1016/S0144-8617\(02\)00183-2](https://doi.org/10.1016/S0144-8617(02)00183-2)
- <sup>19</sup> I. Pavasars, J. Hagberg, H. Borén and B. Allard, *J. Polym. Environ.*, **11**, 39 (2003), <https://doi.org/10.1023/A:1024267704794>
- <sup>20</sup> T. Hosoya, M. Bacher, A. Potthast, T. Elder and T. Rosenau, *Cellulose*, **25**, 3797 (2018), <https://doi.org/10.1007/s10570-018-1835-y>
- <sup>21</sup> A. Streitwieser, Jr. and C. H. Heathcock, "Introduction to Organic Chemistry", Macmillan Inc., 1976, pp. 698-699, <https://www.macmillanlearning.com>
- <sup>22</sup> Q. Li, A. Wang, W. Ding and Y. Zhang, *BioResources*, **12**, 1263 (2017), <https://doi.org/10.15376/biores.12.1.1263-1272>
- <sup>23</sup> C.-L. Yu and T.-N. Wu, *Int. J. Sci. Eng.*, **5**, 1 (2015), [https://doi.org/10.6159/ijse.2015.\(5-3\).01](https://doi.org/10.6159/ijse.2015.(5-3).01)
- <sup>24</sup> C. N. Sawyer, P. L. McCarty and G. F. Parkin, "Chemistry for Environmental Engineering and Science", 5<sup>th</sup> ed., McGraw-Hill Inc., 2003, 752 p., <https://www.mheducation.com>
- <sup>25</sup> A. Potthast, J. Rohrling, T. Rosenau, A. Borgards, H. Sixta *et al.*, *Biomacromolecules*, **4**, 743 (2003), <https://doi.org/10.1021/bm025759c>
- <sup>26</sup> S. Kongruang, M. J. Han, C. I. G. Breton and M. H. Penner, *Appl. Biochem. Biotechnol.*, **113**, 213 (2004), <https://doi.org/10.1385/ABAB:113:1-3:213>
- <sup>27</sup> C. H. Stephens and P. M. Whitmore, *Cellulose*, **20**, 1099 (2013), <https://doi.org/10.1007/s10570-013-9896-4>
- <sup>28</sup> S. Matsuoka, H. Kawamoto and S. Saka, *J. Anal. Appl. Pyrol.*, **106**, 138 (2014), <https://doi.org/10.1016/j.jaap.2014.01.011>